*Articles*

# Structural Characterization of the Copper Site in Galactose Oxidase Using X-ray Absorption Spectroscopy†

Kimber Clark and James E. Penner-Hahn*

*Department of Chemistry, The University of Michigan, Ann Arbor, Michigan 48109-1055*

Mei Whittaker and James W. Whittaker*

*Department of Chemistry, Carnegie-Mellon University, Pittsburgh, Pennsylvania 15213*

*Received June 20, 1994; Revised Manuscript Received August 10, 1994*®

ABSTRACT: X-ray absorption spectroscopy has been used to characterize the local structural environment of the Cu ion in the reductively inactivated, oxidatively activated, and active+substrate oxidation state derivatives of galactose oxidase. In all three cases, the local environment of the Cu is best modeled by a single shell of low-$Z$ (N or O) scatterers. This is generally consistent with the structure determined crystallographically, although the EXAFS bond lengths are slightly, but significantly, shorter than those found crystallographically. The best-fit average bond lengths are 1.97, 1.95, and 1.98 Å for inactive, active, and active+substrate, respectively. The $Cu^{II}$ ion in the active and inactive derivatives has an apparent coordination number of 4, consistent with the equatorial ligation seen crystallographically. The $Cu^{I}$ ion in the reduced+substrate derivative appears to have either a lower coordination number or a significantly more distorted local environment. The observed $Cu^{I}$–(N/O) bond length favors a model where the Cu becomes 3-coordinate in the substrate–reduced complex.

Galactose oxidase is an extracellular copper-containing enzyme secreted by the fungus *Dactylium dendroides* (Avigad et al., 1962; Whittaker, 1994) that catalyzes the 2-electron oxidation of primary alcohols by $O_2$, yielding the corresponding aldehyde and $H_2O_2$:

$$RCH_2OH + O_2 \rightarrow RCH{=}O + H_2O_2 \qquad (1)$$

The native enzyme has been studied extensively by many researchers over the past 2 decades. Characterization of the active site using EPR, optical absorption, and circular dichroism spectroscopies has given insight into the basic ligand environment of the copper site. The EPR[1] spectrum for native galactose oxidase is characteristic of type 2 Cu(II) proteins and is consistent with oxygen and/or nitrogen being coordinated to the copper in a pseudo-square-planar geometry (Bereman & Kosman, 1977; Kosman et al., 1980). These studies suggested that the copper is coordinated by imidazole and water ligands.

An unusual feature of galactose oxidase is its ability to catalyze a two electron oxidation, despite having only a single monomeric copper site. In general, enzymes lacking additional cofactors contain one redox active metal ion per redox equivalent. The recent development of mild chemical treatments for preparing homogeneous derivatives of the different galactose oxidase derivatives has permitted more detailed spectroscopic characterization of the different oxidation states (Whittaker & Whittaker, 1988). Three oxidation state derivatives of galactose oxidase have been identified: oxidatively activated, reductively inactivated, and active+substrate. Of these, only the reductively inactivated enzyme shows an EPR signal characteristic of Cu(II). The observation of similar Cu(II) ligand field and charge transfer spectra in both inactive and oxidatively activated enzymes demonstrates that the Cu remains Cu(II), despite the loss of the Cu(II) EPR signal (Whittaker & Whittaker, 1988). This oxidation state assignment was subsequently confirmed by X-ray absorption near-edge structure (XANES) spectroscopy (Clark et al., 1990). On the basis of the XANES spectra, the Cu is present as Cu(II) in reductively inactivated and oxidatively activated galactose oxidase and as Cu(I) in the active+substrate form.

These studies support a model in which the 2-electron catalysis utilizes both Cu and a redox active amino acid. In this mechanism, the active oxidized enzyme contains a cupric ion antiferromagnetically coupled to a stable organic radical. Strong antiferromagnetic coupling of these two $S = 1/2$ systems then accounts for the EPR-silent character of the oxidized enzyme.

A recent 1.7 Å X-ray crystal structure of galactose oxidase (Ito et al., 1991) has confirmed the spectroscopic ligand assignments and has provided basic information on the geometric structure of the active site. The copper ligation sphere can be described as a distorted square pyramid. In the equatorial plane there are two histidine imidazoles and one

† This work was supported in part by the NIH (GM-38047 to J.E.P.-H. and GM-46749 to J.W.W.) and by an NIH training grant to K.C. X-ray absorption spectra were measured at the Stanford Synchrotron Radiation Laboratory and the National Synchrotron Light Source, both of which are supported by the U.S. Department of Energy. In addition, SSRL and beam line X9-A at NSLS were supported by NIH Research Resource grants.

* Authors to whom correspondence should be addressed.

® Abstract published in *Advance ACS Abstracts,* October 15, 1994.

[1] Abbreviations: EXAFS, extended X-ray absorption fine structure; EPR, electron paramagnetic resonance; XAS, X-ray absorption spectroscopy; XANES, X-ray absorption near-edge structure; SSRL, Stanford Synchrotron Radiation Laboratory; NSLS, National Synchrotron Light Source; BBDHp, 1,7-bis(2-benzimidazolyl)-2,6-dithiaheptane.

0006-2960/94/0433-12553$04.50/0 

tyrosine, all showing normal Cu(II)–ligand distances. The remaining equatorial site is occupied by a second tyrosine at an unusually long distance (2.59 Å). The approximate square pyramid is completed by an axial water at an even longer distance (2.89 Å). At low pH in acetate buffer, the water is replaced by acetate, which appears to occupy an equatorial site in the anion complex. Spectroscopic studies support this pseudorotation mechanism for the interchange of axial and equatorial sites on binding exogenous ligands (Whittaker & Whittaker, 1993). The crystal structure has revealed a novel covalent modification of one of the copper ligands: a cross-link between a tyrosine residue and a cysteinyl side chain from a remote part of the polypeptide chain. This tyrosine-cysteine dimer is a likely candidate for the protein redox site that stabilizes the organic free radical that is involved in catalysis (Whittaker & Whittaker, 1990; Babcock et al., 1992). This modified tyrosine appears to retain an equatorial position in the inactive enzyme copper complex, both in the presence and absence of exogenous ligands.

X-ray crystallography and X-ray absorption spectroscopy (XAS) give complementary information on protein structure. Although crystallography provides information about the actual atomic arrangement in space, X-ray absorption spectroscopy continues to be the method of choice for the determination of metal–ligand distances in metalloproteins. Where crystallography provides detailed information about protein architecture, XAS yields precise distance information about the local metal atom environment. X-ray absorption spectroscopy has the additional advantage of allowing the enzyme sample to be measured in solution, rather than in the crystalline state. We report extended X-ray absorption fine structure (EXAFS) data for the oxidatively activated as well as the reductively inactivated and active+substrate modifications of galactose oxidase.

## EXPERIMENTAL SECTION

*Preparation of Galactose Oxidase Samples.* Galactose oxidase samples were prepared as previously described (Whittaker & Whittaker, 1988) in 50 mM $Na_2HPO_4$ at pH 7. Enzyme concentrations were 2.0–2.1 mM. The substrate–reduced complex was prepared by adding a slight excess of substrate (methyl β-galactopyranoside) to an anaerobic sample of active galactose oxidase. Oxidation state compositions were verified by measuring the EPR spectra for the frozen samples in the EXAFS sample cells.

*X-ray Absorption Spectroscopy.* EXAFS data collection parameters are summarized in Table 1. EXAFS spectra were measured at the Stanford Synchrotron Radiation Laboratory (SSRL) using beam line 7-3 and at the National Synchrotron Light Source (NSLS) using beam line X-9A. Both synchrotrons were operated under dedicated conditions (2.35 GeV and 60–150 mA at NSLS; 3.0 GeV and 40 mA at SSRL). Data were measured as fluorescence excitation spectra, using a multielement Ge detector array. Samples were placed in Mylar-windowed Lucite cuvettes, and the sample temperature during data collection was held fixed at either 77 K using a home-built liquid nitrogen cold-finger (NSLS) or 10 K using an Oxford Instruments liquid He flow cryostat (SSRL). Data were measured on two independent samples of each galactose oxidase derivative.

Both beam lines utilized a double-crystal monochromator with either Si(111) or Si(220) crystals (see Table 1). At SSRL, harmonic rejection was accomplished by detuning the monochromator to decrease the incident beam intensity by 50%. At NSLS, a harmonic rejection mirror was used and the beam was fully tuned.

Table 1: Data Collection Parameters

| sample | facility | monochromator | temperature (K) |
|---|---|---|---|
| inactive | NSLS | Si(111) | 77 |
| active | NSLS | Si(111) | 77 |
| active+substrate 1 | NSLS | Si(111) | 77 |
| inactive 2 | NSLS | Si(220) | 77 |
| active 2 | NSLS | Si(220) | 77 |
| active+substrate 2 | SSRL | Si(220) | 10 |

EXAFS data reduction followed standard procedures for preedge removal and spline background subtraction (Scott, 1985). An internal Cu foil reference was used to calibrate X-ray energies, with the first inflection point of the foil set to 8980.3 eV. Data were converted to $k$-space, $k = 2\pi/\lambda = (2\, m_e(E - E_o)/\hbar^2)^{1/2}$, with $E_o$ initially defined as 9000 eV. All Fourier transforms were calculated using $k^3$-weighted data over the range 3–13 Å$^{-1}$.

Quantitative interpretation of the data was performed using a nonlinear least sequences minimization of the function, $F = (\sum_{i=1}^{N} k^6(\chi_{calc} - \chi_{obs})^2/(N-1))^{1/2}$, where $N$ is the number of data points and $\chi_{calc}$ and $\chi_{obs}$ are calculated and experimental EXAFS, respectively. The EXAFS spectra were modeled using

$$\chi(k) = \sum \frac{N_s A_s(k)}{kR_{as}^2} \exp(-2k^2\sigma_{as}^2) \exp(-2R_{as}/\lambda(k)) \times \sin(2kR_{as} + \phi_{as}(k)) \quad (2)$$

where $R_{as}$ is the absorber scatterer distance, $N_s$ is the number of scattering atoms (the coordination number), $\sigma_{as}$ is the mean-square deviation in $R_{as}$, the so-called Debye–Waller factor, $\lambda(k)$ is the mean-free path of the photoelectron, $\phi_{as}(k)$ is the phase shift that the photoelectron wave undergoes when passing through the potentials of the absorbing and scattering atoms, and $A_s(k)$ is the back-scattering amplitude function. The expression is summed over all of the shells of scattering atoms, where a shell consists of one or more scatterers at a single (average) distance from the absorber.

The back-scattering amplitude and phase functions were obtained initially as empirical parameters based on EXAFS data for the model compounds $Cu^{II}$cyclam$(SC_6F_5)_2$ (Addison & Sinn, 1983), $Cu^{I}$BBDHp (Schilstra et al., 1982), and $Cu^{II}$(14-ane-S4) (Rorabacher et al., 1983). In this approach, the empirical amplitude function is $A_s(k)\exp(-2k^2\sigma_{as2}) \times \exp(-2R_{as}/\lambda(k))$, and only the change in $\sigma^2$ between the model and the unknown can be determined. Subsequent calculations utilized the ab initio amplitude and phase functions obtained from the program FEFF 3.25. The latter functions were calibrated by adjusting $\Delta E_o$ and a scale factor so as to give the best fit to the crystallographically characterized model compounds. Identical results were obtained using either set of parameters. Fits were done to both the Fourier-filtered ($R$ = 0.9–2.0 Å) and unfiltered EXAFS. Identical bond lengths and Debye–Waller factors were obtained, although the fit quality ($F$) was significantly better for the filtered data.

## RESULTS

The EXAFS spectra for reductively inactivated, oxidatively activated, and active+substrate derivatives of galactose oxidase are shown in Figure 1. The corresponding Fourier transforms of the EXAFS spectra are shown in Figure 2. All three derivatives show similar first shell environments. For each sample, the Fourier transforms are dominated by a peak at approximately 1.8 Å due to copper–nearest neighbor scat-

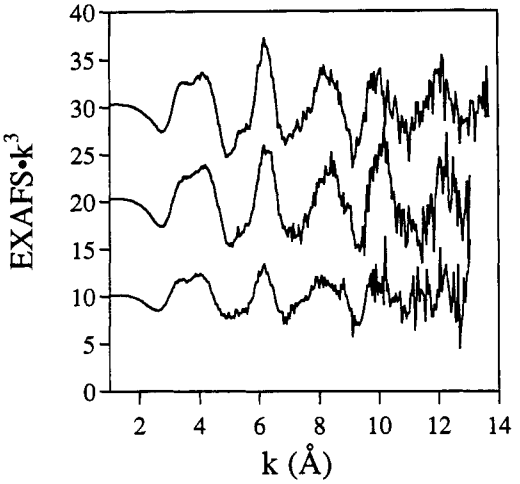


FIGURE 1: EXAFS spectra for galactose oxidase redox modifications. From top: inactive, active, active+substrate. Spectra are weighted by $k^3$ to enhance oscillations at high $k$. All spectra are plotted on the same scale and offset vertically by 30, 20, and 10, respectively, for clarity.

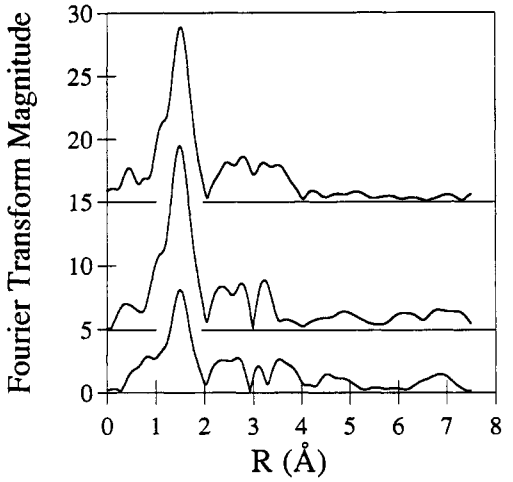


FIGURE 2: Fourier transforms of the data shown in Figure 1. From top: inactive, active, active+substrate. Fourier transforms were calculated using $k^3$-weighted data over the $k$ range 3–13 Å$^{-1}$. All spectra are plotted on the same scale and offset vertically by 15, 5, and 0, respectively, for clarity.

tering. In addition to the first shell peak, the Fourier transforms for all three galactose oxidase derivatives show peaks at longer distances. Most likely, the higher $R$ peaks arise from the outer shell scattering from imidazole scatterers, consistent with the two equatorial histidine ligands seen in the crystal structure. In the following, the outer shell data are not used in the quantitative analysis.

The data shown in Figures 1 and 2 are for sample 2 for each derivative. Comparable first shell data were observed for sample 1 for each derivative. However, the sample 1 spectra (not shown) included an additional signal (ca. 5% of the total fluorescence) corresponding to Cu metal from the cryostat. This contamination has no effect on the first shell EXAFS, since the Cu–Cu peak is well resolved from the first shell scatterer peak; however, the Cu contamination does prevent analysis of the outer shell data for these spectra.

Table 2 summarizes the curve-fitting results for each of the galactose oxidase data sets. For each sample, the first shell was best fit using a single shell of low-$Z$ scatterers. The best fits for the Cu(II) derivatives were obtained for a coordination number of ca. 4, as required by the crystal structure. In unknown structures, it is difficult to determine the true

Table 2: Curve-Fitting Results for Filtered First Shell Data

| sample | no. | $N$ | $R$ (Å) | $\sigma^2$ (Å$^2$ × 10$^3$) |
|---|---|---|---|---|
| active | 1 | 4 | 1.96 | 4.7 |
| | 2 | 4 | 1.95 | 1.0 |
| inactive | 1 | 4 | 1.97 | 6.3 |
| | 2 | 4 | 1.97 | 1.6 |
| active+substrate | 1 | 3 | 2.00 | 8.1 |
| | 2 | 4 | 1.98 | 6.9 |
| | 2 | 3 | 1.98 | 4.1 |

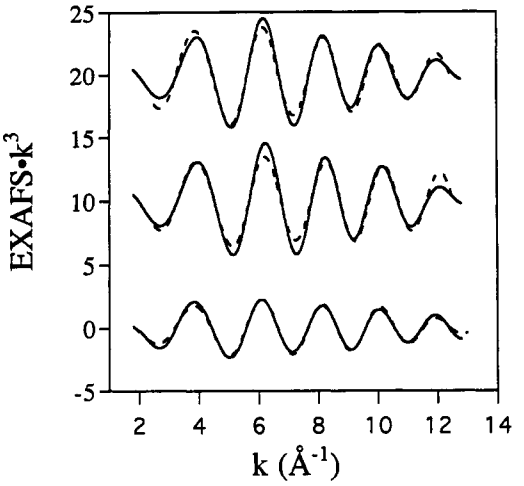


FIGURE 3: Best fit to Fourier-filtered first-shell data for (from the top) inactive, active, and active+substrate galactose oxidase. For each spectrum, the data are shown as the solid lines, and the best single shell fits are shown as the dashed lines. All spectra are plotted on the same scale and offset vertically by 20, 10, and 0, respectively, for clarity.

coordination number using EXAFS, since coordination number and Debye–Waller factor are highly correlated. However, since the true coordination is known for galactose oxidase, this can be fixed and the EXAFS data can be used to obtain a measure of the disorder in the Cu site (i.e., the Debye-Waller factor). Fourier back-transformed (filtered) spectra corresponding to the first shell for each enzyme form are shown in Figure 3. Back-transformed spectra are shown with their corresponding best fit.

No significant improvement was observed if two shells of (O/N) scatterers were used instead of a single shell. This does not mean that all of the Cu–(O/N) distances are identical, but rather that they cannot be divided into two shells within the resolution limits of the present data (ca. 0.15 Å).

## DISCUSSION

The average first shell bond length is slightly longer in the inactive form (1.98 Å) than in the active form (1.96 Å). These bond lengths are both significantly shorter than those reported for the equatorial ligands in the crystal structure (2.12, 2.24, 1.91, 2.59; average, 2.21 Å). This deviation appears to exceed the reported uncertainty in the crystallographic distance (0.15 Å). For a structure having three ligands at a relatively short distance (average = 2.09 Å) and a fourth at a much longer distance, the EXAFS would most likely reflect only the three shorter ligands. Even here, the average EXAFS bond length is significantly shorter than that seen crystallographically. Moreover, the small EXAFS Debye–Waller factor is inconsistent with the large spread of distances reported crystallographically. Three ligands at 2.12, 2.24, and 1.91 Å would give $\sigma^2 \approx 6 \times 10^{-2}$ Å$^2$, compared to the observed values of (1–5) × 10$^{-3}$ Å$^2$. The differences between the EXAFS and the crystallographic distances may reflect either the difference

between the form of the enzyme (EXAFS, frozen solution; crystallography, room temperature crystal) or the uncertainties inherent in the different structural probes. With regard to possible structural changes, it is noteworthy that galactose oxidase shows thermochromic behavior that has been interpreted in terms of deprotonation of the bound water and displacement of one of the tyrosine ligands (Whittaker & Whittaker, 1993). It is thus likely that the EXAFS spectra, measured at low temperature, are sampling a form of the enzyme different from that which was crystallized.

In analyses of the EXAFS, the Cu–ligand scattering has been modeled using Cu–N scattering. Attempts to fit the data using a mixture of Cu–O and Cu–N scatterers at ca. 2 Å were unsuccessful. One of the two shells refined to a chemically unrealistic Debye–Waller factor, the refined bond lengths were separated by less than the resolution of the EXAFS (ca. 0.15 Å), and there was no significant improvement in the fit quality. This indicates that the spread in Cu–(N/O) distances must be small, and is consistent with the small Debye–Waller factors found in the fits. Fits using Cu–O scatterers in place of Cu–N scatterers give comparable fits, with an apparent average bond length that is 0.02–0.03 Å shorter due to the additional phase shift for Cu–O scattering. Since the actual ligation environment contains a mixture of N and O scatterers, the true distance is probably 0.01–0.02 Å shorter than the distances reported in Table 2. This correction will have no effect, however, on the relative bond lengths for the different oxidation state derivatives.

The 1.96–1.98 Å Cu–(N/O) bond length is typical of those found for 4-coordinate Cu(II) complexes (Alcock et al., 1987; Knapp et al., 1987, 1990). In particular, it is substantially longer than the average Cu–(N/O) bond length of 1.81–1.83 Å found for 4-coordinate Cu(III) complexes (Diaddario et al., 1983; Anson et al., 1987). This confirms our earlier conclusion, based on the edge energies, that both the inactive and active forms of galactose oxidase contain a divalent copper.

The decrease in Cu–(N/O) bond length following redox activation is small but reproducible. Although the estimated accuracy in EXAFS bond lengths is ca. ±0.02 Å, the precision for comparing two similar structures is much better, ca. ±0.005 Å. The difference in bond lengths between inactive and active galactose oxidase is thus likely to represent a real structural change. The bond length contraction may reflect the increase in ligand field interactions when the overall charge on the complex is reduced by oxidation of the Cys-Tyr dimer. The net charge of Cu + ligands + Cys-Tyr dimer shifts from 0 to +1 upon redox activation. It has been suggested that this increase in ligand field may account for the 10-fold higher anion affinity of the active enzyme compared to the inactive form (Whittaker & Whittaker, 1993), and it could also account for the slight decrease in the average Cu–(N/O) bond length.

The crystal structure for galactose oxidase shows an axial water ligand at ca. 2.81 Å from the copper. We see no evidence for an additional scatterer at 2.6–2.8 Å in fits to the unfiltered EXAFS data. Although it is possible to include O/N scatterers at approximately this distance, such scatterers have unrealistically large Debye–Waller factors (20–70) × $10^{-3}$ Å$^2$) and do not significantly improve the fit. This is not surprising given the long Cu–O(water) distance; there are numerous examples of distant ligands that are not EXAFS detectable (Scott et al., 1982; Penner–Hahn et al., 1989). The lack of EXAFS-detectable scattering can arise either from a very weak interaction (i.e., uncorrelated motion of the Cu and the water oxygen) or from interference between scattering from the water oxygen and other long distance scatterers (e.g., the imidazole carbon shell at ca. 3 Å).

The cysteine sulfur from the cross-linked Tyr-Cys dimer does not appear to be coordinated to Cu in the crystal structure (crystallographic Cu–S distance, 3.51 Å). Recent model studies show that analogous thioether linkages in model compounds can coordinate to Cu and that a consequence of coordination is a pyramidalization at S. The planar geometry of the cysteinyl side chain in the protein structure reinforces a nonligating role for sulfur in this complex (Whittaker et al., 1993). However, the geometry of the active site could plausibly permit formation of a Cu–S bond in one or more of the galactose oxidase oxidation states. No evidence for sulfur ligation is seen in the EXAFS. As with the water oxygen, however, the absence of a detectable Cu–S signal does not rule out sulfur coordination, although it does rule out the formation of a strong (ca. 2.3 Å) Cu–S bond.

Upon the addition of substrate to galactose oxidase, the copper is reduced to Cu(I) and the first shell bond length increases slightly to 1.99 Å. The increase is relatively small, compared to that expected for the decrease in oxidation state. Several lines of evidence suggest that the short Cu(I) bond length is the result of a decrease in the Cu coordination number upon reduction. A survey of the Cambridge Crystallographic Database[2] for $Cu^I$–(N/O) complexes gives average bond lengths of 1.98 Å for 3-coordinate complexes and 2.04 Å for 4-coordinate complexes. The observed bond length for reduced galactose oxidase is thus most typical of those found in 3-coordinate Cu–(N/O) complexes, although a 4-coordinate site cannot be ruled out on the basis of bond length alone. The EXAFS amplitudes are also consistent with a 3-coordinate Cu(I) site. There is an obvious decrease in FT amplitude on reduction (Figure 2), the EXAFS data are fit somewhat better by a 3-coordinate model (see Table 2) and the 3-coordinate model gives a more reasonable Debye–Waller factor. Although these observations favor a 3-coordinate Cu(I), they could be consistent with a distorted 4-coordinate Cu in reduced galactose oxidase. Finally, the XANES spectrum for reduced galactose oxidase [see Figure 1 of Clark et al. (1990)] shows a pronounced 1s→4p transition at ca. 8984 eV. The intensity and energy of this transition are characteristic of 3-coordinate Cu(I) complexes and significantly different from those seen in 4-coordinate Cu(I) (Kau et al., 1987).

The formation of a 3-coordinate cuprous complex is consistent with the reductive mechanism previously outlined for galactose oxidase (Whittaker & Whittaker, 1993), in which the unmodified tyrosine is displaced and the product carbonyl is effectively unbound, leaving only three groups bound to Cu: two histidine imidazoles and the modified tyrosine residue.

## CONCLUSIONS

The average Cu–ligand bond lengths in frozen solutions of inactive, active, and active+substrate galactose are consistent with the known structures for Cu(II) and Cu(I) complexes, respectively. These numbers significantly differ from those seen crystallographically, although at least part of this variation appears to be due to the different states of the enzyme for the different measurements. The EXAFS-derived bond lengths support a mechanism where the Cu becomes 3-coordinate following the binding of substrate and reduction to Cu(I).

[2] A total of 35 3-coordinate and 91 4-coordinate Cu(I) complexes were identified as having ligation consisting of a single shell of N/O scatterers. No distinction was made for ligation type or charge. Within a given coordination number, the standard deviation in the average bond length is ca. 0.04 Å.

## REFERENCES


Addison, A. W., & Sinn, E. (1983) *Inorg. Chem. 22*, 1225–1228.

Alcock, N. W., Lin, W.-K., Jircitano, A., Mokren, J. D., Corfield, P. W. R., Johnson, G., Novotnak, G., Cairns, C., & Busch, D. H. (1987) *Inorg. Chem. 26*, 440–452.

Anson, F. C., Collins, T. J., Richmond, T. G., Santarsiero, B. D., Toth, J. E., & Treco, B. G. R. T. (1987) *J. Am. Chem. Soc. 109*, 2974–2979.

Avigad, G., Amaral, D., Asensio, C., & Horecker, B. L. (1962) *J. Biol. Chem. 237*, 2736–2743.

Babcock, G. T., El-Deeb, M. K., Sandusky, P. O., Whittaker, M. M., & Wihittaker, J. W. (1992) *J. Am. Chem. Soc. 114*, 3727–3734.

Bereman, R. D., & Kosman, D. J. (1977) *J. Am. Chem. Soc. 99*, 7322–7325.

Clark, K., Penner-Hahn, J. E., Whittaker, M. M., & Whittaker, J. W. (1990) *J. Am. Chem. Soc. 112*, 6433–6434.

Diaddario, L. L., Robinson, W. R., & Margerum, D. W. (1983) *Inorg. Chem. 22*, 1021–1025.

Ito, N., Phillips, S. E. V., Stevens, C., Ogel, Z. B., McPherson, M. J., Keen, J. N., Yadav, K. D. S., & Knowles, P. F. (1991) *Nature 350*, 87–90.

Kau, L. S., Spira-Solomon, D. J., Penner-Hahn, J. E., Hodgson, K. O., & Solomon, E. I. (1987) *J. Am. Chem. Soc. 109*, 6433–6442.

Knapp, S., Keenan, T. P., Zhang, X., Fikar, R., Potenza, J. A., & Schugar, H. J. (1987) *J. Am. Chem. Soc. 109*, 1882–1883.

Knapp, S., Keenan, T. P., Zhang, X., Fikar, R., Potenza, J. A., & Schugar, H. J. (1990) *J. Am. Chem. Soc. 112*, 3452–3464.

Kosman, D. J., Peisach, J., & Mims, W. B. (1980) *Biochemistry 19*, 1304–1308.

Penner-Hahn, J. E., Murata, M., Hodgson, K. O., & Freeman, H. C. (1989) *Inorg. Chem. 28*, 1826–32.

Rorabacher, D. B., Martin, M. J., Koenigbauer, M. J., Malik, M., Schroeder, R. R., Endicott, J. F., & Ochrymowycz, L. A. (1983) in *Copper Coordination Chemistry: Biochemical and Inorganic Perspectives* (Karlin, K. D., & Zubieta, J., Eds.) pp 167–202, Adenine Press, Guilderland, NY.

Schilstra, M. J., Birker, P. J. M. W. L., Verschoor, G. C., & Reedijk, J. (1982) *Inorg. Chem. 21*, 2637–44.

Scott, R. (1985) *Methods Enzymol. 117*, 414–459.

Scott, R. A., Hahn, J. E., Doniach, S., Freeman, H. C., & Hodgson, K. O. (1982) *J. Am. Chem. Soc. 104*, 5364–5369.

Whittaker, J. W. (1994) in *Metal Ions in Biological Systems* (Sigel, H., & Sigel, A., Eds.) pp 315–360, Marcel Dekker, New York.

Whittaker, M. M., & Whittaker, J. W. (1988) *J. Biol. Chem. 263*, 6074–6080.

Whittaker, M. M., & Whittaker, J. W. (1990) *J. Biol. Chem. 265*, 9610–9613.

Whittaker, M. M., & Whittaker, J. W. (1993) *Biophys. J. 64*, 762–772.

Whittaker, M. M., Chuang, Y.-Y., & Whittaker, J. W. (1993) *J. Am. Chem. Soc. 115*, 10029–10035.